

NON –LINEAR ANALYSIS OF REINFORCED CONCRETE BEAMS STRENGTHENED WITH STEEL AND CFRP PLATES

Ali L. Abbas

Engineering College , Diyala University

ABSTRACT:- Non –linear analysis of reinforced concrete beams strengthened with bonding steel or carbon-fiber reinforcement plates has been investigated in this paper. The ANSYS computer program was used for this purpose. The finite element models are developed using a smeared crack approach for concrete , three dimensional solid elements(solid 65) for concrete, three dimensional solid elements(solid 45) for steel plate ,and three dimensional layered elements(solid 46) for carbon -fiber- reinforced plastic plate(CFRP). Three- dimensional finite element analysis was conducted to obtain the response of the strengthened beams with steel and CFPR plates in terms of applied load -deflection , tension force distribution in the strengthening plates along the reinforced concrete beams, and bond force distribution in the beam with CFRP plate and beam with steel plate. The present study contains six beams, three of them those which are tested by Zarnic et al (1999)which are regarded as case study one and the other three beams are the overhanging beams which are supposed in this study as case study two .One beam for each case study was kept as the control beam while the other two beams were externally strengthened with CFRP and steel plates. Results from the ANSYS finite element analysis are compared with those obtained from experimental results and other available numerical results. The comparisons show good accuracy.

Keywords:- Finite Element Modeling, Reinforced concrete beams, Steel plates, CFPR plates

INTRODUCTION

In the last two decades, the application of fiber reinforced polymers as external reinforcement has received much attention from structural engineering. Community FRP laminates have gained popularity as external reinforcement for the strengthening or

rehabilitation of reinforced concrete structures and they are preferred over steel plate due to their high tensile strength , high strength– weight ratio and corrosion resistance(Agostino Monteleone 2008) ⁽¹⁾ . The use of carbon fiber for structural applications was first studied at the Swiss Federal testing, Laboratories (EMPA) (Meier and Winistorfer1995). Due to many advantage of using FRP plates as external reinforcement ,extensive research has been carried out regarding their performance. Yozhizawa et al (1996)⁽²⁾ examined the effect of various bonding conditions on the bond strength between CFRP sheets and concrete. Chajes et al (1996) ⁽³⁾ investigated the effect of the shear bond strength of FRP plates. Arduini and Nanni (1997) ⁽⁴⁾ conducted a parametric study to investigate the effects of FRP on strength and failure mechanisms of repaired RC beams, the analysis aimed to investigate the effect of FRP parameters such as stiffness, bond length, adhesive stiffness when employed as repair material. An analytical formulation is to predict the ultimate load of CFRP- plated beam due to concrete cover penetration was presented by Ngujen et al (2001) ⁽⁵⁾. Finally, the non – linear analysis of reinforced concrete beams strengthened with steel and CFRP plates was conducted in this study by using a three- dimensional finite element analysis.

BEAMS IN STUDY

Experiments conducted for this study involve some of reinforced concrete beams which are tested at university of Ljubljana ,Slovenia , by Prof. R. Zarnic and coworkers and described in specimen geometry and test layout for beams tested by Zarnic et al (1999) ⁽⁶⁾ which are shown in Fig. (1) as well as a new case study is taken represented by using overhanging beams .

Material mechanical properties for the tested beams(case study 1) and for the overhanging beams(case study 2) were summarized in Table (1).The tested beams which represent case study (1) have length of 3200mm while the other beams which represent case study (2) have the same length with overhang cantilever of 1000 mm length. All beams have the same cross section of 200mm wide * 300mm deep. The reinforcement ratio was set to 0.56% for the beams. Six beams were used in this study. One beam for each case study was kept as the control beam while the other two beams were externally strengthened with CFRP and steel plates. The reinforcement plates were 50mm in wide, 1.2mm thick for CFRP and 4mm thick for the steel plates.

ELEMENTS TYPES AND MATERIALS PROPERTIES

Reinforced Concrete

An eight-node solid element, Solid65, was used to model the concrete. The solid element has eight nodes with three degrees of freedom at each node – translations in the nodal x, y, and z directions. The element is capable of plastic deformation, cracking in three orthogonal directions, and crushing. The geometry and node locations for this element type are shown in Fig.(2) ⁽⁷⁾.

For concrete, ANSYS requires input data for material properties as follows:

- Elastic modulus ($E_c=27$ GPa).
- Ultimate uniaxial compressive strength f_c' .
- Ultimate uniaxial tensile strength (modulus of rupture, $f_r = 0.62\sqrt{f_c'}$ ⁽⁸⁾)
- Poisson's ratio ($\nu =0.2$).
- Shear transfer coefficient (β_t)
- Shear transfer coefficient (β_t) which is represents conditions of the crack face. The value of β_t ranges from 0.0 to 1.0 , with 0.0 representing a smooth crack (complete loss of shear transfer) and 1.0 representing a rough crack (no loss of shear transfer) ⁽⁷⁾. The shear transfer coefficient used in present study varied between 0.3 and 0.4 .
- Compressive uniaxial stress-strain relationship for concrete.

The stress- strain relationship for the concrete model was obtained using the following equations to compute the multilinear isotropic stress- strain curve for the concrete :

$$f_c = \varepsilon E_c \quad \text{for} \quad 0 \leq \varepsilon \leq \varepsilon_1 \quad (1)$$

$$f_c = \frac{\varepsilon E_c}{1 + \left(\frac{\varepsilon}{\varepsilon_1}\right)^2} \quad (2)$$

$$\varepsilon_1 = \frac{2f_c'}{E_c} \quad (3)$$

$$f_c = \varepsilon E_c \quad (4)$$

where:

f_c = stress at any strain ε , psi

ε = strain at stress f_c

ε_0 = strain at the ultimate compressive strength f_c'

The multilinear isotropic stress- strain implemented requires the first point of the curve to be defined by the user . It must satisfy Hooks Law:

$$E = \frac{\sigma}{\varepsilon} \quad (5)$$

The multilinear curves were used to help with convergence of the multilinear solution algorithm.

Fig.(3) shows the stress- strain relationship used for this study and is based on work done by Kachlakev,et al. (2001) ⁽⁹⁾. Point 1, defined as $0.30 f_c'$ is calculated in the linear range equation(4) .Points 2,3,and 4 are calculated from equation (2) with ε_0 **obtained** from equation (3). Strains were selected and the stress was calculated from each strain . Point 5 is defined at f_c' . Crushing occurs at ultimate strain $\varepsilon_{cu} = 0.003-0.005$ (Point 6).

REINFORCING STEEL

Steel reinforcement in the experimental beams was constructed with typical steel reinforcing bars. Properties, i.e., elastic modulus and yield stress, for the steel reinforcement used in this FEM study follow the design material properties used for the experimental investigation. The steel for the finite element models was assumed to be an elastic-perfectly plastic material and identical in tension and compression. Fig.(4)shows the stress-strain relationship used in this study.

Material properties for the steel reinforcement for all three models follow the design material properties used for the experimental investigation.

A Link8 element was used to model the steel reinforcement in this study. Two nodes are required for this element. Each node has three degrees of freedom, – translations in the nodal x, y, and z directions. The element is also capable of plastic deformation. The geometry and node locations for this element type are shown in Fig.(5)⁽⁷⁾.

FRP COMPOSITES

A layered solid element, Solid46, was used to model the FRP composites. The element allows for up to 100 different material layers with different orientations and orthotropic material properties in each layer. The element has three degrees of freedom at each node translations in the nodal x, y, and z directions. The high strength of the epoxy used to attach

the bonding plates to the experimental beams supported the perfect bond assumption. The geometry, node locations, and the coordinate system are shown in Fig.(6) ⁽⁷⁾.

Input data needed for the CFRP composites in the finite element models are as follows:

- Number of layers.
- Thickness of each layer.
- Orientation of the fiber direction for each layer.
- Elastic modulus of the FRP composite in three directions (E_x , E_y and E_z).
- Shear modulus of the FRP composite for three planes (G_{xy} , G_{yz} and G_{xz}).
- Major Poisson's ratio for three planes (ν_{xy} , ν_{yz} and ν_{xz}).

A summary of material properties used for FRP composites used for the finite element modeling of the strengthened beam in the present study is shown in Table (2).

STEEL PLATES

An eight-node solid element, Solid45, was used for the steel plates at the supports in the beam models and loading locations in the finite element models (as in the actual beams) in order to avoid stress concentration problems the element is defined with eight nodes having three degrees of freedom at each node. An elastic modulus of 210GPa and Poisson's ratio of 0.3 were used in this study follow the design material properties used for the experimental investigation). The geometry and node locations for this element type are shown in Fig. (6) ⁽⁷⁾.

ANALYSIS OF RESULTS

In this study simple representation by using ANSYS computer program for each beam are shown in figures (8),(9), (10) (11),(12), (13) and due to symmetrical nature of Zarnic specimens only half of the beams span which represent case study 1 are modeled while the overhanging beams which represent case study 2 are modeled using the whole spans of the beams.

In figures (14) ,(15) and (16), the results obtained from finite element analysis by using ANSYS computer program are compared with experimental and other available numerical results⁽¹⁰⁾ in which two-noded displacement- based reinforced concrete beam element is used and a fine mesh is used along the beam in order to obtain accurate and detailed results ,for the beams in terms of applied load -midspan deflection. The finite element model yields a good estimate of both stiffness and and the strength of all beams. for all beams the finite element model is stiffer than the actual beam in the linear range. Perfect bond between the concrete

and steel reinforcing is assumed in the finite element analyses, but the assumption would not be true for the actual beams. As bond slip occurs, the composite action between the concrete and steel reinforcing is lost. Thus, the overall stiffness of the actual beams could be lower than what the finite element models predict, due to factors that are not incorporated into the models.

A few meaningful points are labeled on the curves. Point *c* marks the onset of concrete cracking in the middle third of the beam and is followed by a drop in the beam stiffness. Point *E* represents a generic point during loading at which cracking spreads toward the beam support but the bottom steel rebars are still elastic. At point *Y_b* the bottom steel rebars yield, leading to a further drop in the response stiffness. *Y_p* indicates the point where the plate steel yields for the case of the RC beams strengthened with the steel plate. As expected, the plate yields (point *Y_p*) before the longitudinal reinforcement yields (point *Y_b*).

After the longitudinal reinforcement yields in the steel-strengthened and in the control beams, the response stiffness is very small and mainly due to the hardening properties of the reinforcement steel. On the contrary, for the beam strengthened with CFRP plate, after point *Y_b* the response stiffness is still considerable because of the elastic contribution of the strengthening plate. At point *D* plate debonding occurs as shown in Fig.(16). A large drop in beams strength because of the loss of the plate contributions can be shown. The residual strength is that of the original, nonstrengthened RC beams.

Strengthening plate force distribution for beams with CFRP plate and steel plate are shown in Fig. (17) and Fig. (18) respectively. According to Fig.(17), the plate force slope has large discontinuities at two locations, at plate end and at loaded point. The discontinuity at the plate end is caused by change in the beam cross section, with plate force jumping from zero at plate end to an almost constant value in the middle third of the beam where the bending moment is constant. Under the point load, the plate force increases rapidly because the plate carries more of tensile force after reinforcing steel yield in the area of maximum moment. The steel yield penetration arrives at point *y_b*, at which the plate force changes slope because the CFRP has to carry any increase in tension once the steel yields. With increasing of load, *y_{yield}* penetration extends till it reaches to the distribution labeled *D* at which debonding occurs.

From Fig. (18), we can obtain that the force in the steel plate can't increase after yielding and the force maximum value is reached at load level *Y_p* whereas the force in the CFRP plates keeps increasing until debonding occurs at load level *D* Fig.(17).

Fig.(19) shows the bond force distribution for the case of CFRP strengthened beam. The bond force is essentially the derivative of the plate force. The plate ends and the loaded point show spikes in the bond force due to sudden change in cross section at the plate end and due to sudden drop in the plate tensile force outside the region of constant moment. Gradual decreases in the bond force distribution can be shown in this figure except at these two locations of discontinuities. The plate force keeps increasing after yielding of steel reinforcement takes place. This yielding doesn't penetrate rapidly. Sharply increasing in the plate force next the point of load application occurs causing a strong bond force around the point of load application, at which the bond force peak equals the epoxy resin strength, followed by decreasing up to point c at which bond force drops to almost zero. We can also show a short plateau of almost constant bond after the peak of the bond force distribution. Thus, debonds in this case starts near the point of load application before the plates reach its ultimate strength.

From Fig(20) it is observed that the bond force for the case of beam strengthened with steel plate is set to zero near the load application point and reaches its maximum value at the plate end. With increasing of load, the yield penetration of steel plates happens and extends from point of load application towards the plate end. Finally, as the bond force reach the epoxy resin strength, debonding starts at plate end with progression of a horizontal splitting crack. Debonding takes place after the external steel plate yielded and reached its ultimate strength. Thus, the beam shows a ductile response due to yielding of steel plate.

Fig.(21) and Fig(22) show the load –deflection curve for case study2 at two locations, the first one at 1.23m from left support and the second at free end. From these figures, the larger stiffness increase obtained with steel plate rather than with the CFRP plates mainly because the steel plate axial stiffness is more than twice the stiffness of the CFRP plate.

CONCLUSIONS

1. The general behavior of the finite element models represented by the load-deflection plots at midspan show good agreement with the experimental results and other available numerical results. However, for all beams which represent case study one, the finite element model show slightly more stiffness than the actual beams in the linear range due to excluding the effects of bond slip (between the concrete and steel reinforcing) and micro cracks occurring in the actual beams which lead to the higher stiffness of the finite element models.

2. The average strength for all beams which represent case study one and case study two with steel plate shows larger increasing than the average strength for the beams strengthened by means of CFRP plates because the steel plate axial stiffness is more than twice the stiffness of CFRP.
3. A further difference can be notice between the behaviour of the CFRP strengthening plate and the steel strengthening plate. The plate force keeps increasing after yielding of steel reinforcement takes place. This yielding doesn't penetrate rapidly. Sharply increasing in the plate force next the point of load application occurs causing a strong bond force around the point of load application whereas, for the case of the steel strengthening plate, yielding of the external plate takes place first and propagates from the load application point along the beam pushing the bond force localization toward the plate end .
4. From results, we can also obtain that the ultimate failure condition for all strengthened beam is due to debonding of the strengthened plates which always starts near the point of load application before the plates reaches its ultimate strength for the case of CFRP strenthened beams and the strengthened beams in this case show a brittle behaviour, while debonding for the case of beams strengthened with steel plate takes place after the external plates yielded and reached its ultimate strength . The strengthened beams for this case show a ductile response due to yeilding of steel plate.

REFERENCES

- 1- Monteleone,A. (2008)“ Numerical Analysis of Crack Induced Debonding Mechanisms in FRP-Strengthened RC Beams "M.Sc. thesis, Department of Civil Engineering, University of Waterloo. P.P 256.(Cited)
- 2- Yoshizawa, H., Myojo, T., Okoshi, M., Mizukoshi, M., and Kliger, H. “Effect of Sheet Bonding Condition on Concrete Members Having Externally Bonded Carbon Fiber Sheet. Materials for the New Millennium:Proceedings of the Fourth Materials Engineering Conference, 2, 1608-16.
- 3- Chajes, M. J., Finch, W. W., Jr., Januszka, T. F., and Thomson, T. A., Jr. (1996). “Bond and force transfer of composite material plates bonded to concrete.” ACI Struct. J., 93(2), 208–217.

- 4- Arduini, M., and Nanni, A. (1997). “ Parametric Study of Beams with Externally Bonded FRP Reinforcement. " ACI Structural Journal, 94, 5, 493-01 .
- 5- Ngujen, D.M., Chan, T.K., and Cheong, H.K. (2001). “Brittle Failure and Bond Development Length of CFRP-Concrete Beams" Journal of Composites for Construction, 5, 1, 12-17.
- 6- Zarnic, R., Gostic, S., Bosiljkov, V., and Bokan-Bosiljkov, V. (1999). “Improvement of Bending Load-Bearing Capacity by Externally Bonded Plates " Specialist Techniques and Materials for Concrete Construction, Proceedings of the International Conference on Creating with Concrete, 433-42.
- 7- "ANSYS Manual" ,Version 9.0 .
- 8- ACI 318m-05, American Concrete Institute,(2005) Building Code Requirements for Reinforced Concrete, American Concrete Institute, Farmington Hills, Michigan.
- 9- Kachlakev,D.I.,Miller, T.,Yim, S., Chanswat, K., Potisuk,t. (2001)"Finite Element Modeling of Reinforced Concrete Structures Strengthened with FRP Laminates" Final Report for Oregon Department of Transportation .(Web Site).
- 10- Alessandra Aprile et al (2001) “Role of Bond in RC Beams Strengthened with Steel and FRP plates"Journal of Structural Engineering .P.P 1445.

NOMENCLATURE

• Ultimate uniaxial compressive strength	f_c'
• Concrete elastic modulus	E_c
• Steel elastic modulus	E_s
• Stress at any strain ϵ	f_c
• Concrete modulus of rupture	f_r
• Shear transfer coefficient	β_t
• Strain at stress f_c	ϵ
• Strain corresponding to $(0.3 f_c')$	ϵ_1
• Ultimate compressive strain	ϵ_{cu}
• Strain at the ultimate compressive strength	ϵ_o
• Poisson’s ratio	ν

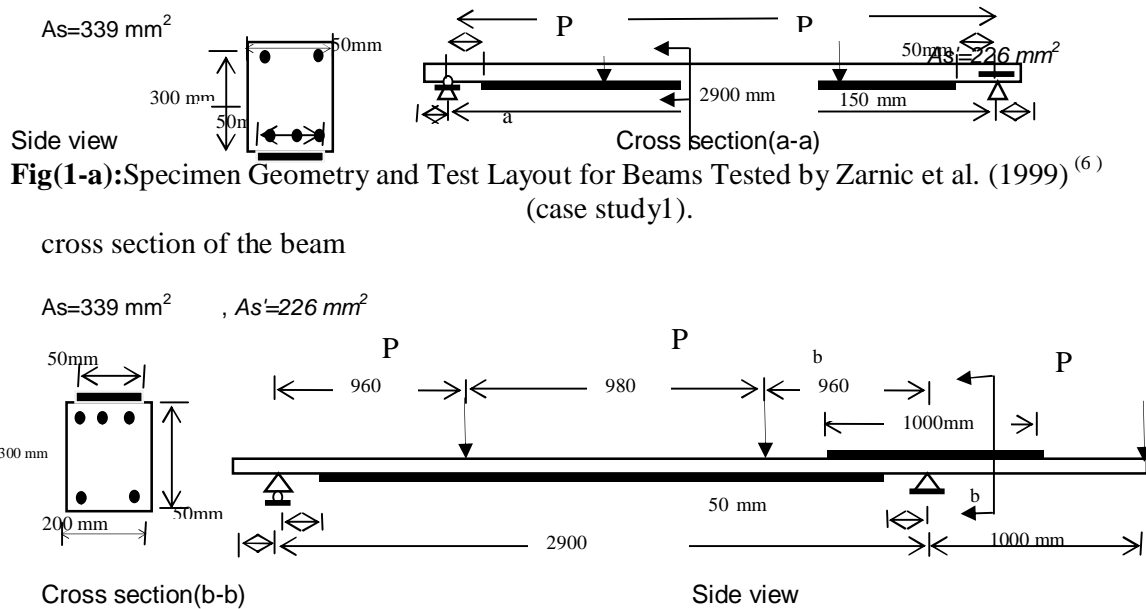
Table(1) :Summary of material Properties Used by Zarnic et al (1999)⁽⁶⁾(case study 1)
 as well as used for(case study 2).

Parameter	Elastic modulus (GPa)	Poisson's ratio	Compressive strength(MPa)	Tensile strength (MPa)
Concrete	27	0.2	25	3.5
Steel bars	210	0.3	460	460
Steel plate	210	0.3	360	360
CFRP plate	150	0.33	–	2,400
Epoxy resin	12.8	0.35	100	4 ^a

^a Adhesion for concrete surface .

Table (2): Summary of material properties for FRP composite.

FRP composite	Elastic modulus N/mm^2	Major Poisson's ratio	Shear modulus N/mm^2
Carbon fiber reinforced	$E_x = 62,000$ $E_y = 4800$ $E_z = 4800$	$\nu_{xy} = 0.22$ $\nu_{xz} = 0.22$ $\nu_{yz} = 0.30$	$G_{xy} = 3270$ $G_{xz} = 3270$ $G_{yz} = 1860$



Fig(1-a):Specimen Geometry and Test Layout for Beams Tested by Zarnic et al. (1999)⁽⁶⁾
 (case study1).

Fig (1-b):New case study by using overhanging beams(case study 2).

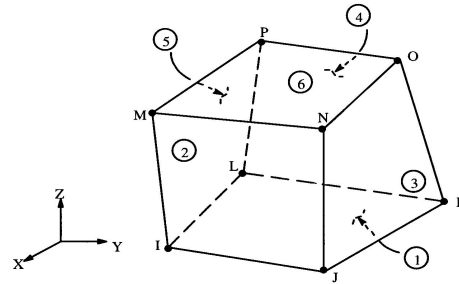


Fig.(2): Solid65 – 3-D reinforced concrete solid⁽⁷⁾.

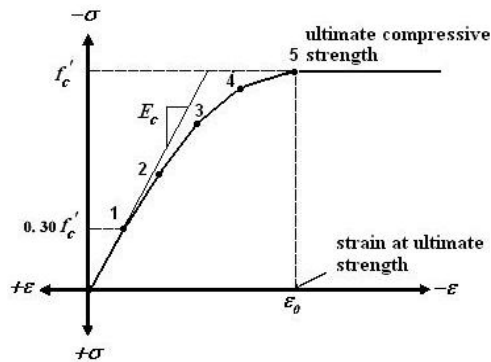


Fig.(3): Stress- Strain Relation Model for Concrete⁽⁹⁾.

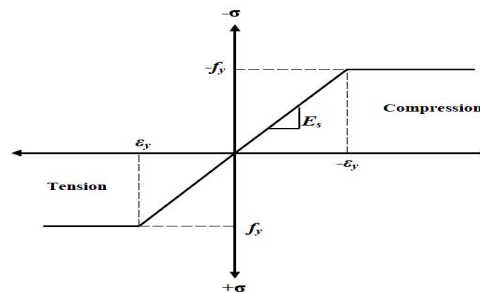


Fig.(4): Stress-strain curve for steel reinforcement.

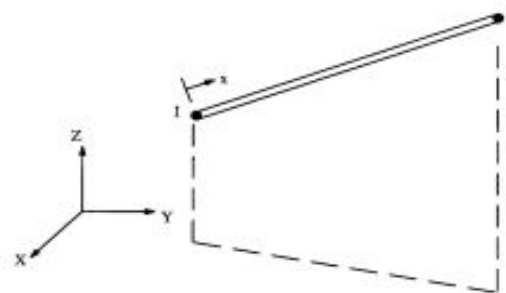
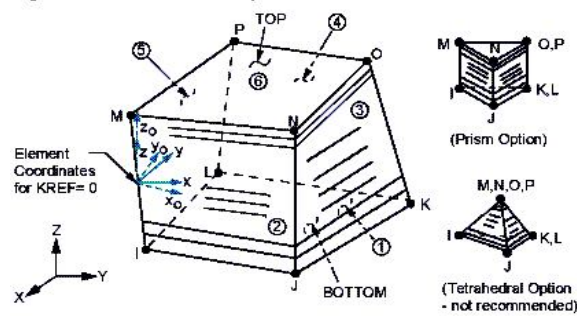


Fig.(5): Link8 element geometry⁽⁷⁾.



x_0 = Element x-axis if ESYS is not supplied.
 x = Element x-axis if ESYS is supplied.

Fig.(6): Solid 46 layered element geometry⁽⁷⁾.

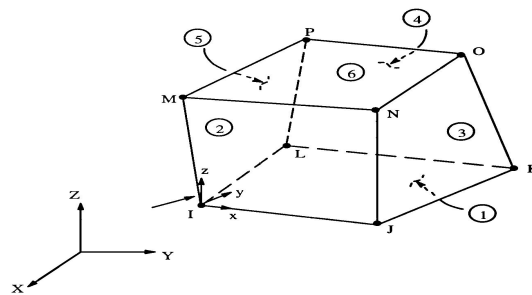
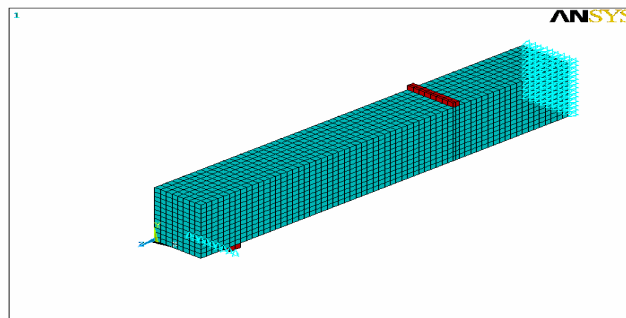
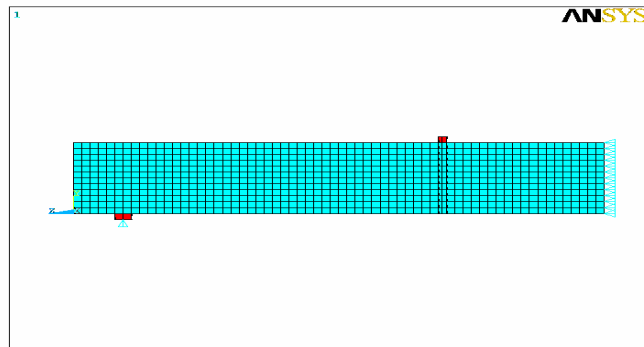


Fig.(7): Solid45 – 3-D Solid⁽⁷⁾.

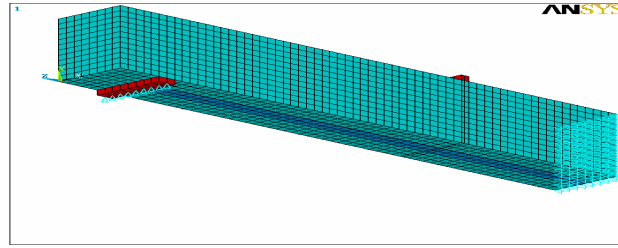


(A)

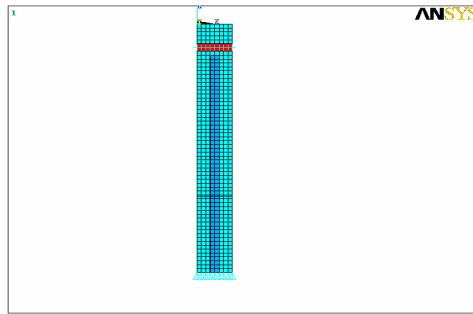


(B)

Fig. (8):Control Beam(Case Study 1) with Boundry Condition in Different views (A)- Iso, (B)- Side.

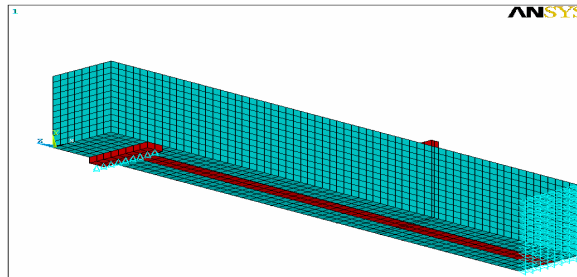


(A)

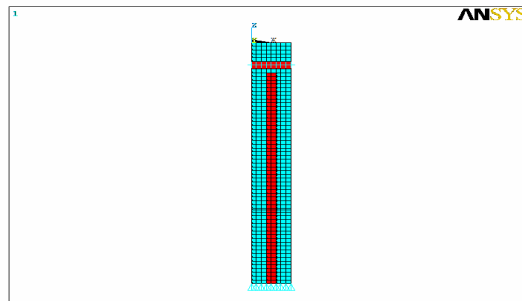


(B)

Fig. (9):CFRP Strengthened Beam(Case Study 1) with Boundry Conditon in Different Views (A)- Iso ,(B)- Bottom.



(A)



(B)

Fig. (10): Steel-Strengthened Beam(Case Study 1) with Boundry Conditon in Different Views (A)- Iso ,(B)- Bottom.

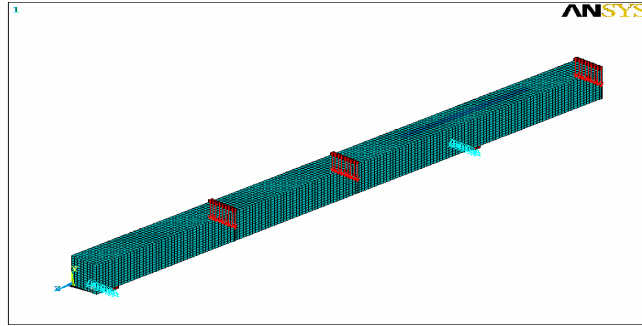


Fig. (12):CFRP Strengthened Beam(Case Study 2) with Boundry Conditon.

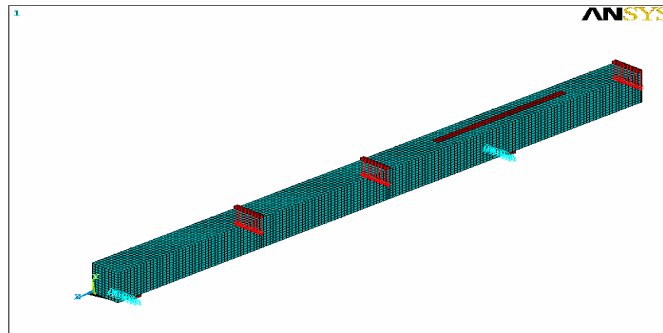


Fig. (13): Steel-Strengthened Beam(Case Study 2) with Boundry Conditon.



Fig.(14):Load- Deflection Curves for Control Beam(Case Study 1).

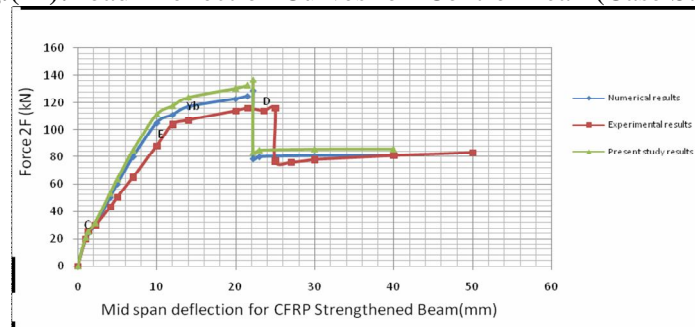


Fig.(15):Load- Deflection Curves for Beam Strngthened with CFRP Plate(Case Study 1).



Fig.(16): Load- Deflection Curves for Beam Strngthened with Steel Plate(Case Study 1).

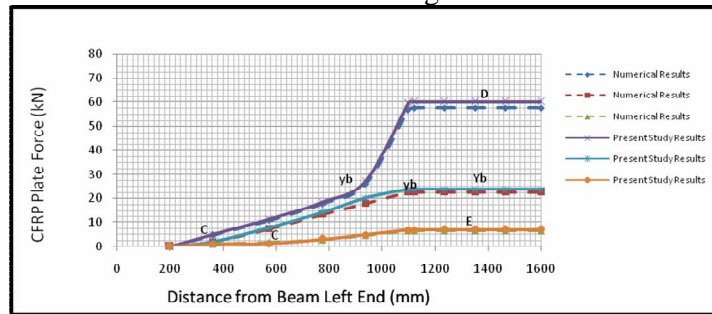


Fig.(17):Strengthening Plates Force Distributions for Beams with CFRP Plate(Case Study 1).

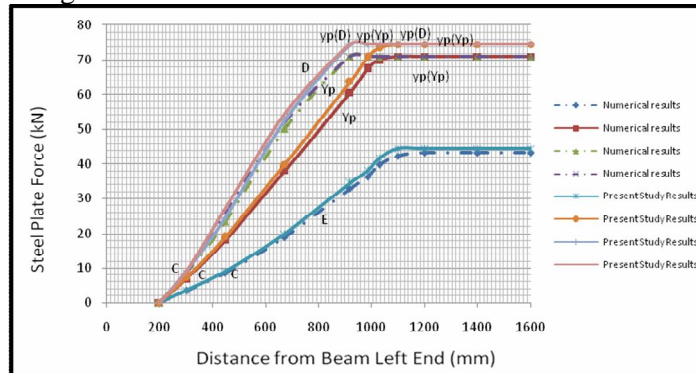


Fig.(18):Strengthening Plates Force Distributions for Beams with Steel Plate(Case Study 1).

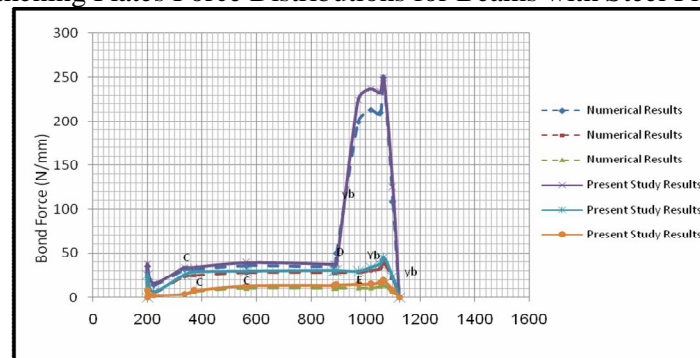


Fig.(19): Bond Force Distributions for Beam with CFRP Plate(Case Study 1).

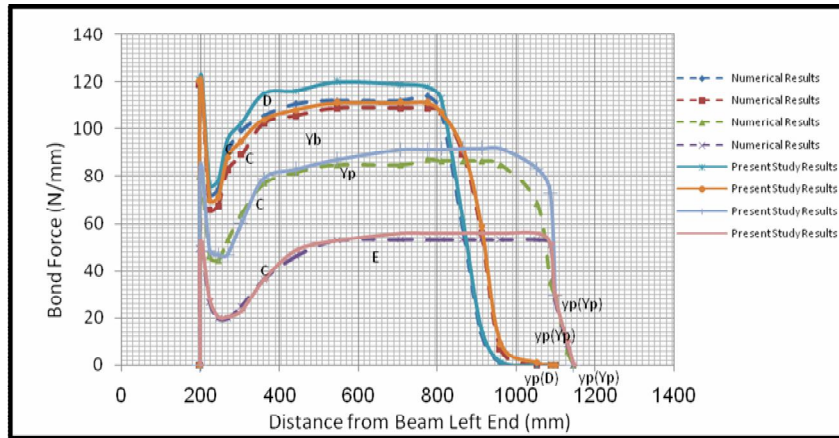


Fig.(20): Bond Force Distributions for Beams with Steel Plate(Case Study 1).

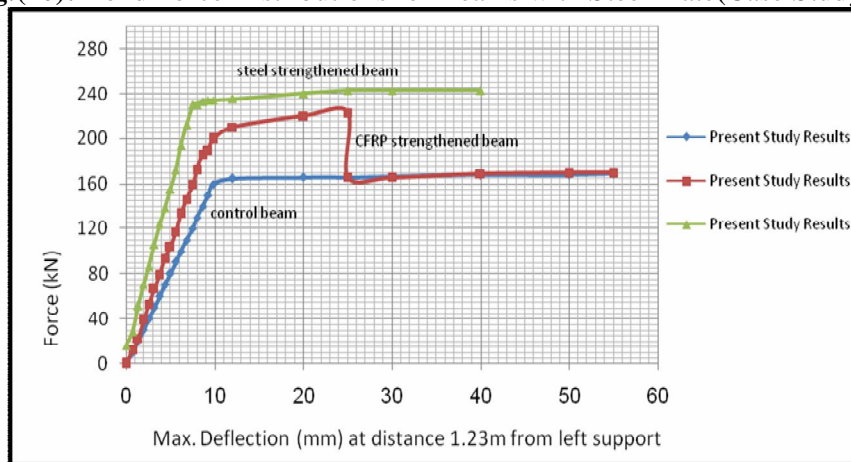


Fig.(21):Load- Deflection Curves for Overhanging Beams at Distance 1.23m from Left Support.

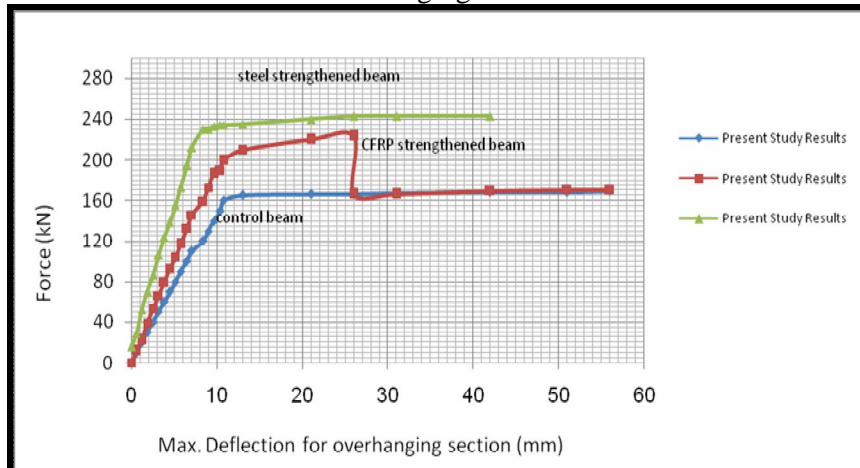


Fig.(22):Load- Deflection Curves for Overhanging Beams(Case Study 2).

السلوك اللاخطي للعتبات الخرسانية باستخدام صفائح الحديد أو بوليمرات الكربون المقواة

د. علي لفته عباس

مدرس

كلية الهندسة . جامعة ديالى

الخلاصة

لقد تم في هذا البحث المختصر دراسة السلوك اللاخطي للعتبات الخرسانية المقواة باستخدام صفائح الحديد او بوليمرات الكربون حيث تم استخدام البرنامج ANSYS لهذا الغرض 0
لقد تم التمثيل لهذه العتبات باستخدام العناصر الصلدة الثلاثية الأبعاد (solid 65) والعناصر الصلدة الثلاثية الأبعاد (solid 45) لتمثيل صفائح الحديد وكذلك الصفائح الطبقيّة الثلاثية (solid46) لتمثيل بوليمرات الكربون حيث تم استخدام طريقة العناصر المحددة لاستنتاج السلوك اللاخطي لهذه العتبات المقواة باستخدام صفائح الحديد او بوليمرات الكربون 0 لقد تم رسم المنحنيات التي توضح العلاقة ما بين الاحمال المسلطة والهطول الحاصل في هذه العتبات, قوى الشد الموزعة على طول هذه العتبات الخرسانية و قوى الربط الموزعة ايضا على طول العتبات الخرسانية المقواة 0 تم استخدام ستة اعداد خرسانية في هذه الدراسة ثلاث عتبات منها ذات اسناد بسيط تلك التي تم فحصها كنماذج عملية من قبل العالم Zarnic وآخرين سنة 1999 والتي تم اعتبارها كحالة دراسة أولى حيث ان العتب الاول لم يتم تقويته اما العتب الثاني فقد تم تقويته باستخدام صفائح بوليمرات الكربون اما الثالث فقد تم تقويته باستخدام صفائح الحديد 0 أما الثالث أعتاب خرسانية المتبقية هي عتبات ذات اسناد بسيط مع طرف نهاية حرة بطول 1م والتي تم اعتبارها كحالة ثانية والتي تم تقويتها بنفس الاسلوب السابق 0 بعض النتائج المستحصلة من البرنامج تم مقارنتها مع النتائج العملية والنتائج الاخرى المتوفرة حيث اظهرت النتائج حالة توافق جيدة 0
الكلمات الدالة: طريقة العناصر المحددة , اعداد خرسانية مسلحة, صفائح الحديد, بوليمرات الكربون.